

# Evaluation of 222 nm vs 254 nm Lamps for In-duct UVGI Air Disinfection: Irradiance Characterization, Inactivation Performance, and Environmental Implications

Jay Patel<sup>1</sup>, Lexuan Zhong<sup>1\*</sup>

<sup>1</sup>Department of Mechanical Engineering, University of Alberta, Edmonton, AB, T6G 1H9, Canada

## Abstract

Challenges remain in characterizing the in-duct irradiance distribution of UVC lamps with air parameters. This study experimentally characterizes irradiance of 222 nm & 254 nm lamps in a conduit using the 9-point average method. Irradiance is measured from all six sides at each point, and a correction factor is proposed to adjust for the overlapped detection angles of a spectrometer. The output of the 254 nm lamp increases by 18% with a rise in air temperature (25°C to 35°C) and decreases by 21% with increased air velocities (0.5 m/s to 2 m/s). In contrast, the 222 nm lamp shows minimal output change with air parameters. Relative humidity variations (25% to 60%) did not affect the output of any lamp. While the 222 nm lamp operation in stagnant air leads to ozone generation, the total volatile organic compound levels exhibit minimal change. Finally, UVGI experiments targeting *E. coli* inactivation efficiency are conducted for both lamps, suggesting 254 nm lamp as a more cost-effective & sustainable solution for continuous in-duct air disinfection.

## Introduction

The COVID-19 pandemic has underscored the critical need to prevent the transmission of airborne pathogens within indoor environments, where individuals often spend prolonged periods. While conventional approaches such as increasing ventilation rates and utilizing high-efficiency filters have shown some effectiveness, they present challenges in terms of energy consumption and economic viability (Nunayon, Zhang, and Lai 2020). Historically employed for water disinfection, Ultraviolet Germicidal Irradiation (UVGI) systems offer an alternative solution to the limitations of traditional methods for mitigating airborne pathogens. UV light, which covers the electromagnetic spectrum of 100 nm to 400 nm, is classified as UVA (320-400 nm), UVB (280-320 nm) and UVC (200-280 nm) for disinfection purposes (Guerrero-Beltrán and Barbosa-Cánovas 2004). Among them, UVC has the highest genetic damage capability to the microorganisms such as virus, bacteria, fungi and spores (Yaun et al. 2004). Upon interaction with UVC photons, DNA molecules undergo photochemical reactions, forming pyrimidine dimers within

the DNA strands. This process inhibits DNA replication and transcription, ultimately resulting in cell death of microorganisms (Franz et al. 2009).

Based on their application, the UVGI air disinfection system can be characterized as Upper-room system, a Whole-room system, and an In-duct system (Nunayon, Mui, and Wong, 2023). This study specifically focuses on UVGI in-duct air disinfection applications, the performance of which primarily depends on the type of UV wavelength, UV irradiation distribution, UV exposure time to bioaerosols, and susceptibility of microorganisms to UV wavelength (Luo and Zhong 2021). UV exposure time is mainly dependent on the air velocity, while the susceptibility of microorganisms mostly relies on the inherent biological properties of microorganisms, which cannot be changed. Sometimes, air parameters like relative humidity (RH) can also affect the susceptibility of the microorganism. However, the most important parameter from an engineering perspective is UV irradiation distribution, coupled with exposure time. The type of UV lamp used, UV lamp arrangement, duct dimensions and duct material can potentially affect the UV irradiation distribution trend in addition to air operating parameters like air temperature and air velocity (Luo and Zhong 2021). Therefore, understanding, and accurate mapping of the actual irradiation field present inside the duct is essential for avoiding the poor in-duct UVGI system design.

Characterizing detailed irradiation trends often involves simulations using trigonometric functions, with the lamp assumed as a line or point source, or employing a view factor approach, both commonly utilized by researchers (Luo and Zhong 2022). However, these methods necessitate complex engineering calculations and costly computational resources, which may not be feasible in practical applications. An alternative approach involves experimental measurement of irradiation using instruments such as radiometers, spectrometers, photometers, or chemical actinometers at designated locations. Although disinfection within the duct or chamber is a volumetric phenomenon, most of the available sensors measure irradiance in a planner way. In the duct, where reflections from the side walls are significantly high, it becomes necessary to account the

irradiation from all six sides (Luo and Zhong 2021). Some studies only measured irradiations from single side leading to underestimation, while others simply added the irradiation from all six sides, without considering the angle detection limit of the sensor used, potentially resulting in overestimation of average irradiation (Nunayon, Zhang, and Lai 2020; Wang et al. 2023; Zhang and Lai 2022a).

Traditionally, the 254 nm low-pressure mercury lamp (LP) is widely used and studied. The irradiation of a 254 nm lamp has been observed to vary with the operating conditions, primarily with air temperature and velocity (Luo and Zhong 2021). While one study noted a change in the output of a 254 nm lamp with different relative humidity (RH) levels (Zhang et al. 2020), another study found no such correlation (Lau, Bahnfleth, and Freihaut 2009). The mercury used inside the LP lamp is hazardous to human health in case the lamp breaks. In addition, the UVC light at 254 nm degrades human health (skin and eye damage) upon exposure to it. As a safer alternative, the use of 222 nm far UVC-filtered excimer lamps is currently gaining popularity. Studies have found that 222 nm does not penetrate inside the human skin, making it safe for exposure (Zhang and Lai 2022b). In addition, some studies showed concerns regarding the ozone level and total volatile organic compounds (TVOC) generated by the excimer lamps (Graeffe et al. 2023). Moreover, detailed life cycle assessment comparing the cost-effectiveness, energy efficiency, & sustainability of both lamps for disinfecting specific microorganisms is needed. *E.coli*, the most commonly found bacteria in various environments, has been selected to compare the disinfection performance of both lamps in the duct.

Overall, this paper aims to characterize and compare 222 nm and 254 nm lamps by (1) experimentally assessing irradiance distribution using a novel correction factor, (2) analyzing the impact of air temperature, velocity & RH on the lamp output, (3) evaluating ozone & total volatile organic compound (TVOC) generation levels by both lamps, & (4) compare cost-effectiveness, energy efficiency and sustainability for *E.coli* air disinfection in duct.

## Material & Method

### Pilot scale in-duct UVGI system

A pilot-scale stainless steel duct system with cross-sectional dimensions of 12.7 cm × 12.7 cm was developed in accordance with the specifications outlined in ASHRAE Standard 185.1–2020 for in-duct UVGI disinfection experiments. The system comprises essential components like fans, UV lamps, mixing baffle, filters, injection, and sampling ports, as depicted in Fig. 1. To regulate air parameters (velocity, temperature, and relative humidity) within the duct system, a feedback control system (Opto 22) was installed. Additionally, for uniform injection and sampling of aerosols, a cross-shaped probes were installed with each probe consisting of four branches and five sampling holes per branch. Pre-qualification tests, including leakage, velocity, and aerosol uniformity, were conducted

to align with ASHRAE Standard 185.1–2020, the comprehensive results of which are provided elsewhere (J. Wu, Luo, and Zhong 2022).

### UVC Lamps: Installation & Characterization

The UVC low-pressure mercury lamp (OSRAM GCF5DS, 5 W X 1) and far-UVC filtered excimer lamps (Cure-UV 510100-20, 20 W X 2) with peak wavelengths of 254 nm & 222 nm respectively were installed as depicted in Fig.2. Both UVC lamps are installed in the same x-y plane, that distribute the total UV exposure length (116.3 cm) into two sections: upstream (47.5 cm) & downstream (68.8 cm). The single 254 nm mercury lamp (Ø12 mm) is installed at the centre of the plane, while two cylindrical tubes of 222 nm lamps (Ø 35 mm) are installed symmetrically.

The UVC irradiance ( $\text{mW}/\text{cm}^2$ ) of both lamps was measured using a recently calibrated spectrometer (ILT 960; International Light Technologies, Peabody, MA, USA) with input optics RAA4. The device has  $\pm 15\%$  &  $\pm 10\%$  uncertainty in the measurement of 222 nm and 254 nm lamps, respectively. Irradiance measurements were conducted on five vertical planes that are parallel to the light bulbs and perpendicular to the directed airflow as depicted in Fig. 3 (a). The irradiance measurements were taken on the downstream side, and the principle of symmetry was used for the upstream side. Each vertical plane was divided into  $3 \times 3$  grids, as depicted in Fig. 3 (b), and a 9-point average method was used to characterize the irradiance of each plane. While it is essential to measure irradiance from all six sides due to potential reflections from the duct walls, the preliminary test revealed that irradiance contribution from the side facing opposite to the lamp is negligible. Thus, during measurement, the light detector was positioned at the center of each grid, and irradiance from only 5 sides (front, left, right, top & bottom) was measured in this study. Lamp start-up time is also observed for both lamps using the same spectrometer.

Initially, both the lamps underwent a burnt-in period of a minimum of 100 hours before characterizing them under static conditions at room temperature ( $20^\circ\text{C} \pm 1^\circ\text{C}$ ). Subsequently, air velocity was varied from 0.5 m/s to 2 m/s ( $T = 25^\circ\text{C}$  &  $\text{RH} = 40\%$ ) and changes in irradiance were measured from all the sides at downstream planes for both lamps. Similarly, air temperature is varied from  $25^\circ\text{C}$  to  $35^\circ\text{C}$  ( $v=0.5$  m/s,  $\text{RH}=40\%$ ) and Relative Humidity from 25% to 60% ( $v=0.5$  m/s,  $T=25^\circ\text{C}$ ) to evaluate their effects on lamp output. Irradiance was measured thrice under all the mentioned air parameter conditions to ensure the reliability and accuracy of the data over the average fluctuations in the supplied voltage and current.

Finally, both lamps are tested for generation of ozone and total volatile organic compounds (TVOCs). Since the air velocity is likely to dilute their concentration and render them non-detectable, static room air conditions ( $T=20^\circ\text{C}$ ,  $\text{RH}=60\%$ ) were used to measure them. Initially background ozone level and TVOC levels were recorded. Then, the

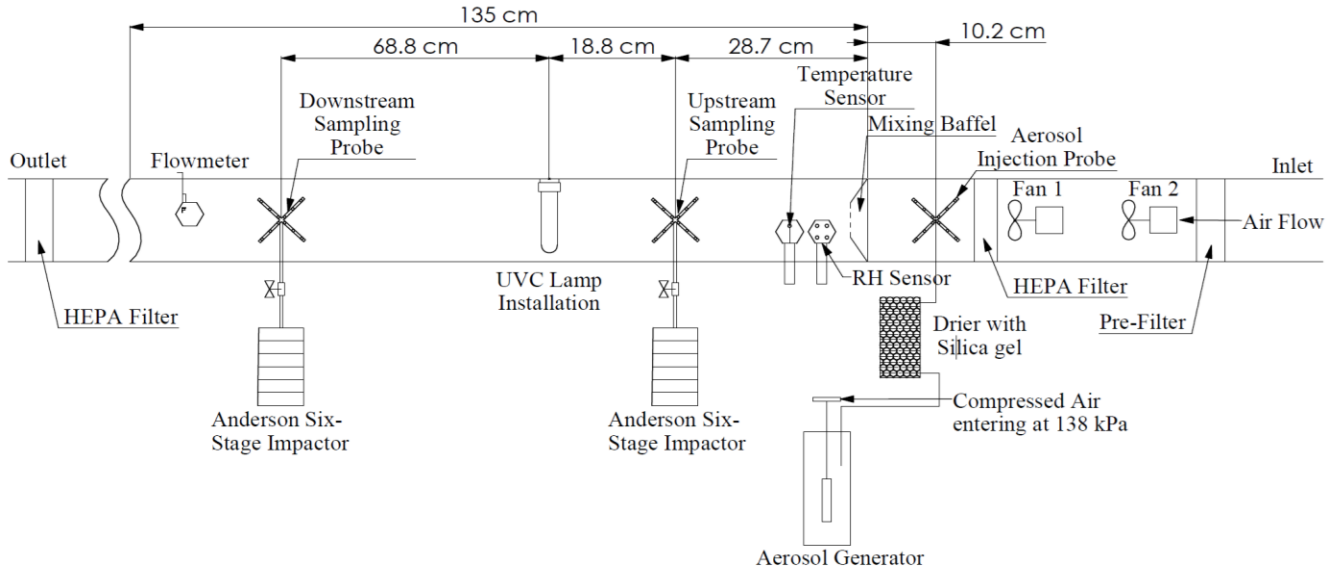


Figure 1: Pilot Scale HVAC duct Setup

lamps were turned on for 30 minutes and average ozone and TVOC levels were continuously monitored for three repetitive sessions. A daily calibrated photoionization detector (PID, HYPERSENSE 1002, HENGAN, China) with resolution of 5 ppb, response time less than 5 s, and error of  $\pm 10\%$  was used to record TVOC levels. The ozone concentration was measured by using an ozone monitor (Teledyne API's Model 465L) with a measuring range of 1 to 1000 ppm, response time less than 30 s, sampling flow rate at 0.8 LPM and error of  $\pm 1\%$ .

### Irradiance Calculation & Correction Factor

Most radiometric measurement devices used for characterizing lamps do not receive light from all 360° angles, necessitating irradiance measurement from multiple sides. However, it is crucial to consider the angle detection limit of the sensors used. For instance, the ILT960 spectrometer employed in this study features diffuser with cosine correction, aiming to capture irradiation from all the 180° angles. However, the ideal cosine response indicates that any sensor below  $\pm 60^\circ$  only measures half or less irradiance than the original value. Moreover, the actual cosine response curve of ILT960 provided by manufacturer depicts more than  $\pm 10\%$  fluctuations from the ideal cosine

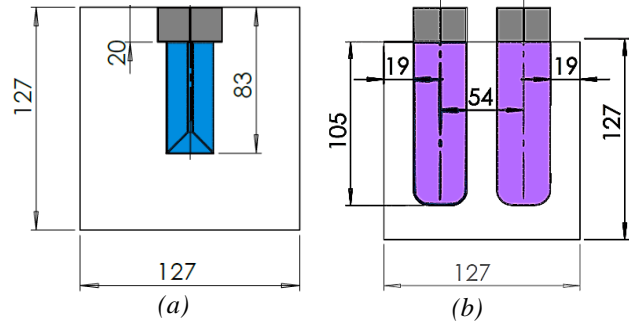


Figure 2: Installation of lamps; (a) 254 nm, (b) 222 nm. All dimensions are in mm.

values, making the measured readings unreliable beyond those angles. Therefore, it is recommended to consider the angle detection limit of the sensor employed in this study as  $120^\circ$  ( $-60^\circ$  to  $+60^\circ$ ). When irradiance is measured from two adjacent sides, the total  $120^\circ$  detection limit of each side results in  $30^\circ$  overlap of irradiance, which is measured twice as illustrated in Fig 4, potentially leading to overestimation of average irradiance. Although actual irradiance will be non-uniform over the whole  $120^\circ$  measuring range, it is assumed that the total measured irradiance from a side will be uniformly distributed over the

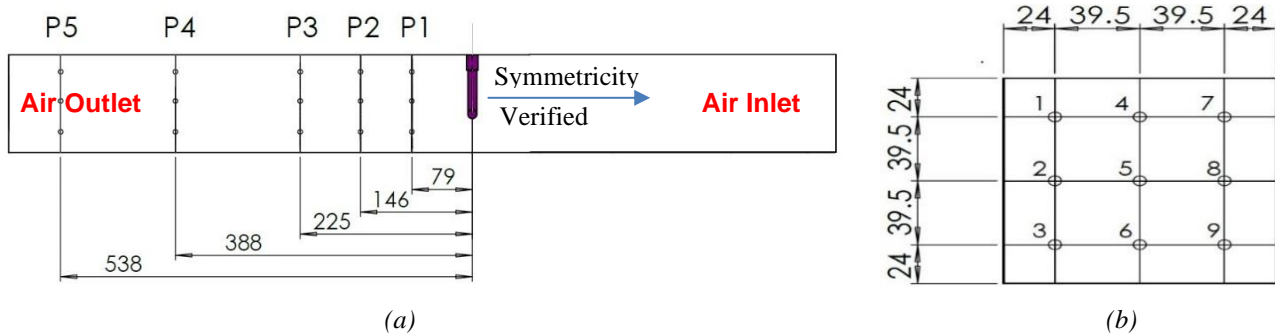


Figure 3: (a) Irradiation measurement planes at downstream; (b) Dimensions of measured grids. All dimensions are in mm.

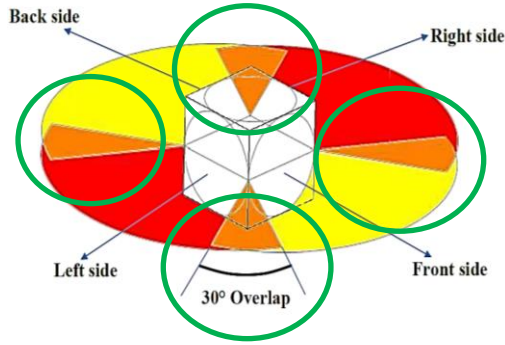


Figure 4: Overlap angle between two adjacent sides

whole measured angles for simplifying the calculations. To address the overestimation issue, a correction factor is introduced in this study, which reduced the measured irradiance of each side in proportion to the overlap angle values for that side as expressed in Eq. 1.

$$C_i = \left(1 - \frac{\phi_1 + \phi_2}{2 * \theta}\right) \quad (1)$$

where,  $C_i$  = Correction factor for irradiance from side,  $i$ ;  $\phi_j$  = Total overlapped angle in measured direction,  $j$  and  $\theta$  =  $2 * \text{Total angle detection limit} = 240^\circ$ .

Finally, the irradiance at a point can be calculated from the following equation.

$$I = C_f I_f + C_l I_l + C_r I_r + C_t I_t + C_b I_b \quad (2)$$

where,  $I$  = Total average irradiance at a specific point;  $I_i$  = Irradiance measured from side,  $i$ ;  $f$  = front side;  $l$  = left side;  $r$  = right side;  $t$  = top side; &  $b$  = bottom side;  $C_f = 0.75$ ;  $C_l = C_r = C_t = C_b = 0.8125$ .

#### UVGI in-duct air disinfection of E.coli

The Escherichia coli (E.coli C3000, ATCC 15597). preparation and sampling procedure is followed those outlined by (Luo and Zhong 2022). In brief, 2% lysogeny broth solution (pH=7.0) was prepared to add the test organism and the suspension culture was then inoculated in a constant temperature shaking incubator (Corning 6750) at 37°C and 170 rpm for 16 to 18 h. Thereafter, the culture was centrifuged at 1750 relative centrifugal force for 15 min and washed three times with 10% phosphate-buffered saline (PBS) solution to harvest E. coli stock. The final pellet was resuspended in 10 mL PBS.

For sampling, aerosols were initially generated from the 50 ml diluted liquid PBS suspension using a 1-jet nebulizer (Collision Nebulizer, BGI) with 138 kPa compressed air in atomizer. These bioaerosols were then injected into duct through an injection tube after passing through dryer. Six-stage Andersen cascade impactors with Glass nutrient agar (NA) Petri dishes between each stage were employed to collect the samples at downstream with vacuum pump (flow rate: 28.3 L/min). Following sample collection, the plates were sealed & incubated overnight at 37 °C for almost 16 to 18 hours. Finally, the number of colonies formed on the plates was counted and converted to the corresponding

corrected particle counts using the positive-hole conversion table(Macher 1989) .

The pilot HVAC system was maintained at the desired operating condition (T: 25°C, v: 0.5 m/s, and RH: 40%), after which the compressed air was turned on for the nebulization process. After 20 minutes of stabilization, the UVC-off samples are collected at downstream. Then, the UVC light is turned on for 15 minutes, and again, samples downstream are collected in the six-stage impactator. The duct was disinfected with 75% ethanol before and after each experiment. Each test is replicated thrice for reliability.

Preliminary tests revealed that the majority of the cultivable bioaerosol particles are recovered in the size range of 0.65-2.1  $\mu\text{m}$ , which refers to stages 5 & 6 of the cascade impactator. Therefore, only data from those two stages are utilized to evaluate the overall disinfection efficiency of both lamps. It can be formulated as shown in Eq. 3.

$$\eta_{UVGI} = \left(1 - \frac{\sum_{s=5}^6 C_{s,UV-ON}}{\sum_{s=5}^6 C_{s,UV-OFF}}\right) \times 100\% \quad (3)$$

where  $\eta_{UVGI}$  = UVGI disinfection efficiency;  $C_{s,UV-ON}$  = Average cultivable bioaerosol concentrations (CFU/m<sup>3</sup>) with UV light is on;  $C_{s,UV-OFF}$  = Average cultivable bioaerosol concentrations (CFU/m<sup>3</sup>) with UVC light off; and  $s$  = impactor stage numbers.

#### Economic & Sustainability Analysis

Both the UVC technology 254 nm and 222 nm have their own advantages. While the 254 nm lamp is traditionally available in the market & has more capability of genome damage, it must be operated continuously for a longer lifespan. Whereas the 222 nm has more protein damage capability and does not harm humans upon exposure. In this era of sustainability, it is important to select an appropriate lamp which is cost-effective and environmentally friendly. To enable the HVAC designer to select the most sustainable UVGI in-duct solution, a comparative economic, energy efficiency and sustainability study of both lamps is made with the target of E.coli inactivation inside the duct to achieve 90% UVGI efficiency.

There are two main costs associated with UVC lamps' life spans: Initial cost and Operating cost. This study does not consider the cost associated with recycling lamps at the end of their life. Each cost is further simplified for comparison per unit output irradiance. The initial cost can be given as follows.

$$\text{Initial cost} = (\text{Lamp buying cost} + \text{Cost of accessories}) \quad (4)$$

Lamp buying cost depends on the manufacturer, type of UVC lamp, rating of UVC lamps, requirement of any fixtures to install the lamp, and so on. Here, it is assumed that there is no additional cost other than buying the UVC lamp. The next step is to calculate the life-time electricity consumption of UVC lamp, which depends on the lifetime of UV lamps. Normally, when the output of UV lamp reduced by 30% compared to its initial value, the lamp is considered failed. Lamp manufacturers refer to this as L70



lifetime hours, which is usually 8000 hours for 254 nm and 9000 to 10000 hours for 222 nm lamp (Care222® Filtered Far UV-C Excimer Lamp Module | Ushio America, Inc. n.d.). For simplicity most of the manufacturer recommends changing both lamps after continuous operation of 1 year, which is 8760 hours.

$$\text{Annual Electricity Consumption (kWh)} = \text{Lifetime (L70) hours} * \text{Rated Wattage (kW)} \quad (5)$$

$$\text{Annual Operational Cost} = \text{Annual Electricity Consumption (kWh)} * \text{Price of Electricity (CAD/kWh)} \quad (6)$$

$$\text{Annual eCO}_2 \text{ generation} = \text{Annual electricity consumption (kWh)} * \text{electricity consumption intensity (eCO}_2\text{/kWh)} \quad (7)$$

Total cost can be calculated as sum of initial cost and annual operational cost. The price of electricity and the equivalent CO<sub>2</sub> generated for producing that electricity varies by regions. Thus, the comparison of cost, and eCO<sub>2</sub> is made for Alberta & British Columbia (Y. Wu and Zhong 2023).

## Results & Discussion

### UV lamps: Irradiance Distribution

The irradiance of both lamps was exclusively measured in the downstream region, with assumption that symmetrical irradiation would follow in the upstream region. The average total irradiation obtained from Eq. (2) at each point was used to characterize the irradiation field of UV lamps. Experimental verification in this study confirmed that within the 3x3 measured grid on vertical plane, irradiation varies linearly with relative error of less than 10% throughout the duct. Therefore, linear interpolation has been used to fully characterize the irradiation level within planes, as seen in Fig. 5(a) & 5(b). It is evident that the plane closest to the lamp (P1) has the highest irradiation in both types of lamps, which was not distributed uniformly. However, as we moved far away from the lamp (P4 & P5), the uniformity of irradiation became more apparent, albeit with a drastic reduction in irradiation levels. In comparison to 254 nm, it was evident that the 222 nm lamp arrangement has more uniform irradiance, suggesting the installation of two lamps in one row for uniform irradiation distribution closer to

lamp. Its evident that even after using two 20 W lamps for 222 nm, the irradiance is still significantly lower than what achieved by only one 5 W of 254 nm, showcasing lower efficiency of 222 nm lamp output and requirement of more lamps to achieve same irradiance as 254 nm. The irradiance fluctuations at the duct walls or corners may demonstrate the limitation of experimental data and underscore the need for more data points to be measured in those regions.

The linear average of irradiance from 9 measured points accurately represents the overall total average irradiance for the vertical plane. Thus, the 1-D plot illustrating irradiance in relation to the distance from the lamp surface is depicted for both lamps in Fig. 6. Notably, reflections from the duct walls significantly contribute to the irradiance, resulting in values higher than those estimated by the inverse square law as claimed by lam manufacturers, and aligning more closely with the inverse law for the duct applications. The experimental modelling of data is further validated with additional measured vertical planes, demonstrating that the power law accurately predicts the irradiance trend throughout the duct and that the relative error between measured and predicted values is less than 10%.

Furthermore, the irradiation values obtained through the new correction factor method have been compared with the CFD results obtained by (Luo and Zhong 2022) for 254 nm lamp stainless steel one-lamp set up. The average irradiance trend obtained by the new correction method and simulation values are in close agreement with each other in Fig. 6(b) with maximum relative error of 15%, affirming the efficacy of the correction ratio used in this study. The Fig. 7 represents the statistical significance of the correction factor. When the irradiance is only measured from one side, then the plane closest to the lamp (P1) underpredicts the irradiance by nearly 31% and achieves accurate measurements only after approximately 37 cm for 222 nm and 17 cm for 254 nm, where the lamps effectively function as point sources for sensors. Conversely, measuring irradiance from all sides without applying the correction factor consistently overestimates irradiance by almost 30%.

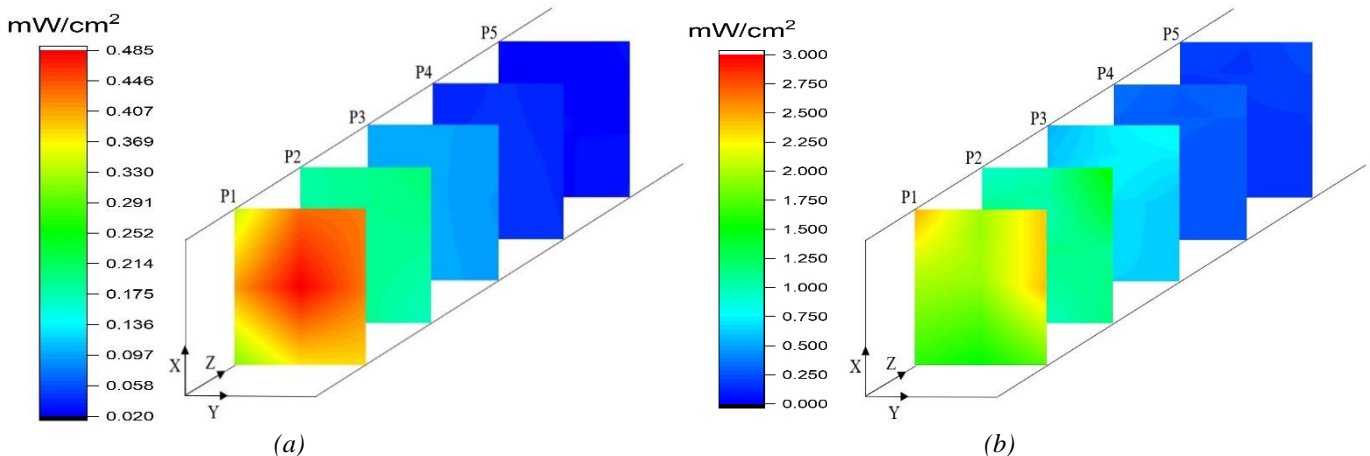


Figure 5: Plane wise measured irradiance distribution (a) 222 nm; (b) 254 nm

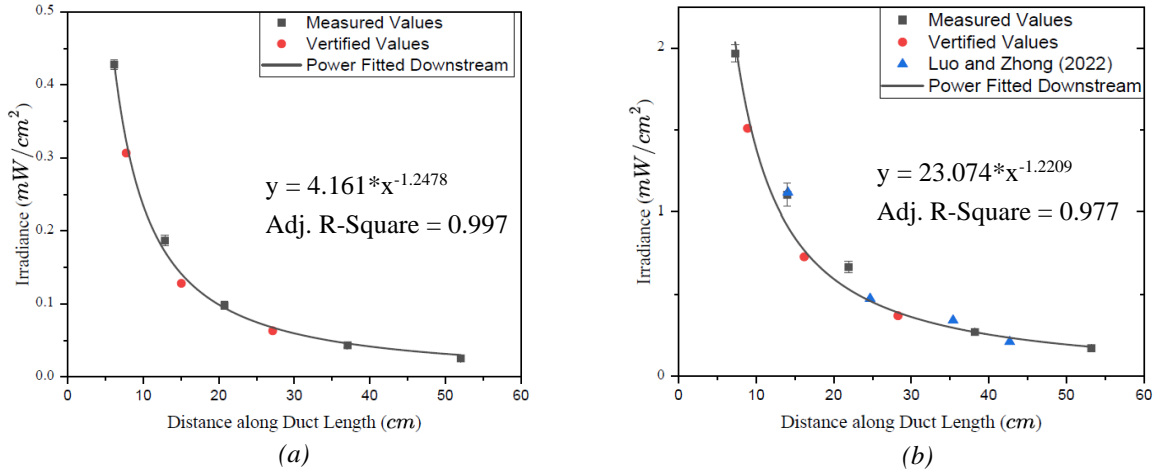


Figure 6: Average Irradiation trend along the duct length (a) 222 nm; (b) 254 nm

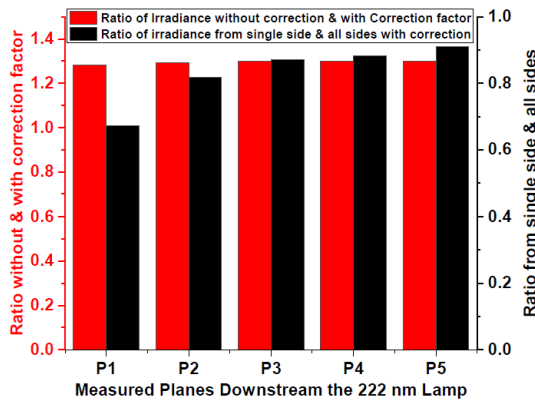


Figure 7: Importance of Correction Factor

Therefore, the use of a correction factor based on the sensor's measuring range is imperative for precisely characterizing lamp irradiance in duct applications.

### UV lamps: Effect of Operating Conditions

The influence of air parameters on lamp output is illustrated in Fig. 8 for both UV lamps. For 254 nm lamps, it is evident that an increase in temperature from 25°C to 35°C results in a significant 18% rise in lamp output. Nonetheless, the rate of increase diminishes when the temperature is raised from 30°C to 35°C, suggesting that beyond 35°C, 254 nm lamps may reach an optimal temperature for maximum output, as confirmed by Lau, Bahnfleth, and Lau, Bahnfleth, and Freihaut, 2009.

Conversely, velocity exhibits an opposite trend: higher velocities correspond to lower lamp output. This phenomenon arises from the wind chill effect generated by higher velocities on the lamp surface temperature, reducing the temperature required for mercury vaporization process. Consequently, as velocity increases, so does the wind chill effect, leading to a decrement in lamp surface temperature and output. This explains the significant drop in mercury lamp output to approximately 80% when the velocity for the 254 nm lamp increases from 0.5 m/s to 2 m/s at a constant

temperature of 25°C. RH levels were not found to affect the output of any lamp.

The 222 nm lamp exhibited no sensitivity to air parameters, attributable to its operational principle. Upon receiving of electricity, the excimer lamp promptly forms excited dimers, transitioning spontaneously from an excited state to a ground state and thus releasing consistent lamp output approximately 4.5 minutes to stabilize its output, whereas the 222 nm lamp initiated within 3 seconds. This variance stems from the differing operational principles of the lamps. The presence of liquid mercury in the 254 nm lamp necessitates vaporization to generate UV light, requiring a warm-up period to reach the vaporization temperature post-startup. Conversely, the 222 nm lamp rapidly forms dimers upon electricity supply, requiring only a few seconds to emit UV light. Regarding ozone generation, the 254 nm lamps did not produce any ozone within a 30-minute sampling period, nor did they generate any levels of total volatile organic compounds (TVOCs). However, the 222 nm far-UVC lamps were found to generate approximately  $2.8 \pm 1.1$  parts per billion (ppb) of ozone over a 30-minute average sampling period at  $18.5 \pm 0.1^\circ\text{C}$  and  $42 \pm 1\%$  relative humidity (RH) due to its operation. This underscores that long term use of 222 nm in a room with limited Air Change per Hour might elevate the ozone in the room. Therefore, ozone-free UV lamps for air disinfection applications needs to be employed in practice. The fluctuation in TVOC levels,

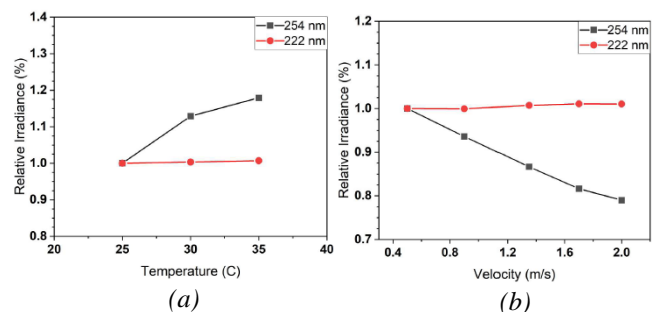


Figure 8: Effect of air parameters, (a) Varying Temperature, (b) Varying Velocity

ranging from 1 to 10 ppb for 222 nm lamp, demonstrates their insignificance.

### E.Coli UVGI Disinfection Efficiency

The airborne E.coli inactivation efficiency was determined at  $0.5 \pm 0.02$  m/s,  $25^\circ \pm 0.3^\circ\text{C}$  &  $40 \pm 3\%$  RH for both 254 nm lamp & 222 nm lamp. The average irradiance measured earlier is  $1.671 \text{ mW/cm}^2$  for 254 nm and  $0.228 \text{ mW/cm}^2$  for 222 nm in the whole duct under a static environment. However, since the output of 254 nm changes with air parameters, the average irradiance at 0.5 m/s,  $25^\circ\text{C}$  & 40% RH should be corrected, as mentioned by (Luo and Zhong 2022), which is almost 94% of the Irradiance measured at static conditions. Therefore, the corrected value of average irradiance at 0.5 m/s,  $25^\circ\text{C}$  & 40% RH is  $1.57 \text{ mW/cm}^2$ .

The disinfection efficiency achieved for the 254 nm is  $99.96\% \pm 0.03\%$ , which is in close agreement with Luo and Zhong (2022), where the similar average irradiance values & velocity was used for E.coli inactivation for the same set-up. For the 222 nm lamps,  $74.5\% \pm 3.1\%$  inactivation efficiency was achieved. These results are compared with Zhang and Lai (2022b), where they have obtained UV rate constant of  $4.9 \text{ cm}^2/\text{mJ}$  for far UVC lamp operated in single pass in-duct application. Based on that, to achieve 74.5% inactivation efficiency with 222 nm for E.coli, the UV dose required is  $0.278 \text{ mJ/cm}^2$ . However, their set up did not include drier and the suspension media used was deionized water. Moreover, their average RH level was 53% during the experiments and their irradiance was not corrected after measuring it from all six sides. These factors lead to significant difference in the value of the UV dose requirement for achieving same efficiency. Therefore, future experiments are targeted to find the UV rate constant for both lamps, which will enable us to compare both technologies under same UV dose, although their output irradiance is different.

### Comparative life cycle analysis of 254 nm Vs 222 nm

Life cycle analysis to attain 90% inactivation efficiency for in-duct E.coli single pass air-disinfection at 0.5 m/s &  $25^\circ\text{C}$  has been performed. In order to do that, UV rate constant of E.coli has been used from the literatures. Luo and Zhong (2022) did similar E.coli disinfection test at 254 nm, and derived UV rate constant as  $5.245 \text{ cm}^2/\text{mJ}$  (40% RH) for same operating conditions. Zhang and Lai (2022b) reported  $4.9 \text{ cm}^2/\text{mJ}$  (53% RH) UV rate constant for 222 nm lamps for duct applications. Based on these values the required dose to achieve the 90 % efficiency is  $0.47 \text{ mJ/cm}^2$  &  $0.44 \text{ mJ/cm}^2$  for 222 nm & 254 nm respectively. Assuming the average exposure time 1 sec, the required average UV dose would be same as the average obtained irradiance.

Table 1 demonstrate the cost and kWh required to achieve the target irradiance for both lamps. It is clearly observed that to achieve the same efficiency, the 254 nm lamp is highly energy efficient, & cost-effective solution. Both the initial cost and the annual kWh require for 254 nm is only

Table 1: Initial cost & kWh of both lamps

| Lamp Type   | 254 nm | 222 nm  |
|---|--------|---------|
| Initial cost, CAD                                       | 44     | 386     |
| Annual kWh  | 43.8   | 350.4   |
| Output, $\text{mW/cm}^2$                                | 1.57   | 0.228   |
| Initial cost, CAD/ $(\text{mW/cm}^2)$                   | 28.02  | 1692.98 |
| Annual kWh/ $(\text{mW/cm}^2)$                          | 27.89  | 1536.84 |
| Initial cost (CAD) to achieve target $(\text{mW/cm}^2)$ | 12.33  | 795.7   |
| Annual kWh to achieve target $(\text{mW/cm}^2)$         | 12.27  | 722.3   |

around 1.6% of that required by 222 nm for continuous operation. Which strongly suggests that 222 nm technology need to be developed further for their cost effectiveness & energy efficiency for 24x7 disinfection applications. Furthermore, the province wise analysis for operational cost and  $\text{eCO}_2$  generation is compared in the Table 2. It demonstrates that for same regions, the total cost and  $\text{eCO}_2$

Table-2: Province wise comparison for sustainability

| Lamp                                 | 222 nm |        | 254 nm |        |
|--------------------------------------|--------|--------|--------|--------|
|                                      | AB     | BC     | AB     | BC     |
| Electricity price, CAD/kWh           | 0.115  | 0.1029 | 0.1155 | 0.1029 |
| Equivalent $\text{gCO}_2/\text{kWh}$ | 640    | 7.8    | 640    | 7.8    |
| Annual kWh req.                      | 722.3  |        | 12.27  |        |
| Operation lifetime cost, CAD         | 83.42  | 74.32  | 1.41   | 1.26   |
| Total cost, CAD                      | 879.1  | 870.02 | 13.74  | 13.59  |
| kg $\text{CO}_2$ produced            | 462.2  | 5.63   | 7.85   | 0.095  |

generation of 222 nm is always going to be higher than the 254 nm lamp, showcasing its low energy efficiency and sustainability. Surprisingly, the 222 nm lamp operated in British Columbia generates less amount of  $\text{eCO}_2$  than the 254 nm lamp operating in Alberta. However, if the lamp handling cost is added after their life, then the excimer lamp may emerge as a more sustainable solution as mercury is toxic and requires special handling treatment. In addition, the 222 nm is more suitable for applications where a continuous on-and-off cycle of a UVC lamp is required, as it does not degrade the life of a 222 nm lamp, unlike the 254 nm lamp. Therefore, the advantage of using different lamps fundamentally lies in the selection of the correct lamps for the correct application. For now, the 254 nm lamp remains a cost-effective, energy-efficient & sustainable solution compared to another UV lamp in the market.

### Conclusion

A novel correction factor method is introduced to fully characterise the irradiance distribution of the 222 nm lamp

and 254 nm lamp inside the duct experimentally. The irradiance is first characterised at static conditions and the resulting average irradiance is verified with simulated values from the literature, ensuring accuracy & reliability of the approach. Based on that it is recommended that angle detection limit of spectrometer used should always be considered and correction should be made for reducing overestimation of irradiance. The varying air parameters did not change the output of 222 nm lamp. RH did not affect the output of any lamps, while temperature and air velocity did significantly affect the output of 254 nm lamp as expected. E.coli in-duct air disinfection experiments showed 99.96%  $\pm$  0.03% efficiency for 254 nm, while 222 nm showed 74.5%  $\pm$  3.1% disinfection. The 222 nm lamp showed extremely high cost and energy consumption for the same disinfection target in comparison with 254 nm, making it less sustainable for continuous operation applications. Future work requires finding UV rate constant for both lamps to compare them under the same UV dose and extension of this framework is required for the UV LEDs available in market.

## References

- “Care222® Filtered Far UV-C Excimer Lamp Module | Ushio America, Inc.” <https://www.ushio.com/product/care222-filtered-far-uv-c-excimer-lamp-module/> (March 28, 2024).
- Franz, Charles M.A.P., Ingrid Specht, Gyu Sung Cho, Volker Graef, and Mario R. Stahl. 2009. “UV-C Inactivation of Microorganisms in Naturally Cloudy Apple Juice Using Novel Inactivation Equipment Based on Dean Vortex Technology.” *Food Control* 20(12): 1103–7.
- Graeffe, Frans, Yuanyuan Luo, Yishuo Guo, and Mikael Ehn. 2023. “Unwanted Indoor Air Quality Effects from Using Ultraviolet C Lamps for Disinfection.” *Environmental Science and Technology Letters* 10(2): 172–78.
- Guerrero-Beltrán, J. A., and G. V. Barbosa-Cánovas. 2004. “Advantages and Limitations on Processing Foods by UV Light.”
- Lau, Josephine, William Bahnfleth, and James Freihaut. 2009. “Estimating the Effects of Ambient Conditions on the Performance of UVGI Air Cleaners.” *Building and Environment* 44(7): 1362–70.
- Luo, Hao, and Lexuan Zhong. 2021. “Ultraviolet Germicidal Irradiation (UVGI) for in-Duct Airborne Bioaerosol Disinfection: Review and Analysis of Design Factors.” *Building and Environment* 197: 107852.
- Luo, Hao, and Lexuan Zhong. 2022. “Development and Experimental Validation of an Improved Mathematical Irradiance Model for In-Duct Ultraviolet Germicidal Irradiation (UVGI) Applications.” *Building and Environment* 226: 109699.
- Macher, Janet M. 1989. “Positive-Hole Correction of Multiple-Jet Impactors for Collecting Viable Microorganisms.” *American Industrial Hygiene Association Journal* 50(11): 561–68.
- Nunayon, Sunday S., Kwok Wai Mui, and Ling Tim Wong. 2023. “Mapping the Knowledge Pattern of Ultraviolet Germicidal Irradiation for Cleaner Indoor Air through the Lens of Bibliometrics.” *Journal of Cleaner Production* 391: 135974.
- Nunayon, Sunday S., Hui H. Zhang, and Alvin C.K. Lai. 2020. “A Novel Upper-Room UVC-LED Irradiation System for Disinfection of Indoor Bioaerosols under Different Operating and Airflow Conditions.” *Journal of Hazardous Materials* 396: 122715.
- Wang, M. H., H. H. Zhang, C. K. Chan, P. K.H. Lee, and A. C.K. Lai. 2023. “Experimental Study of the Disinfection Performance of a 222-Nm Far-UVC Upper-Room System on Airborne Microorganisms in a Full-Scale Chamber.” *Building and Environment* 236: 110260.
- Wu, Jing, Hao Luo, and Lexuan Zhong. 2022. “Development of a Multi-Functional HVAC Facility for the Evaluation of Air Cleaning Technologies and Ventilation Performance.”
- Wu, You, and Lexuan Zhong. 2023. “An Integrated Energy Analysis Framework for Evaluating the Application of Hydrogen-Based Energy Storage Systems in Achieving Net Zero Energy Buildings and Cities in Canada.” *Energy Conversion and Management* 286: 117066.
- Yaun, Brian R., Susan S. Sumner, Joseph D. Eifert, and Joseph E. Marcy. 2004. “Inhibition of Pathogens on Fresh Produce by Ultraviolet Energy.” *International Journal of Food Microbiology* 90(1): 1–8.
- Zhang, Huihui, Xin Jin, Sunday Segbenu Nunayon, and Alvin C.K. Lai. 2020. “Disinfection by In-Duct Ultraviolet Lamps under Different Environmental Conditions in Turbulent Airflows.” *Indoor air* 30(3): 500–511.
- Zhang, Huihui, and Alvin C.K. Lai. 2022a. “Evaluation of Single-Pass Disinfection Performance of Far-UVC Light on Airborne Microorganisms in Duct Flows.” *Environmental sci & technology* 56(24):17849–57.
- Zhang, Huihui, and Alvin C.K. Lai. 2022b. “Evaluation of Single-Pass Disinfection Performance of Far-UVC Light on Airborne Microorganisms in Duct Flows.” *Environmental Science and Technology* 56(24): 17849–57.